Columbia University in the City of New York

LAMONT GEOLOGICAL OBSERVATORY

PALISADES, NEW YORK

ON A DYE DIFFUSION EXPERIMENT OFF LONG ISLAND

Report prepared by: Takashi Ichiye

Technical Report No. CU-9-64 to the Office of Naval Research
Contract Nonr 266(48)

and

Technical Report No. CU-10-64 to the Atomic Energy Commission
Contract AT (30-1)2663

May, 1964

LAMONT GEOLOGICAL OBSERVATORY
(Columbia University)
Palisades, New York

ON A DYE DIFFUSION EXPERIMENT OFF LONG ISLAND

Report prepared by: Takashi Ichiye

Technical Report No. CU-9-64 to the Office of Naval Research
Contract Nonr 266(48)

and

Technical Report No. CU-10-64 to the Atomic Energy Commission
Contract AT (30-1)2663

May, 1964

ABSTRACT

Dye diffusion experiments were made on September 11 and 12 1963 thirty miles south off Long Island. Ten gallons of Rhodamine B dye were pumped at three depths (0, 3m and 7m) in the water each day. On the first day, the dye patch showed a curved pattern and dye was diffused only above 10 meters, perhaps due to rather calm weather conditions. On the second day, the dye patch was elongated but did not show a remarkable curvature; also, dye penetrated into deeper than 70 meters, owing to strong mixing caused by winds of 15 to 20 knots.

In Appendix I, a mathematical model of wind-driven currents in the ocean with a finite depth for eddy viscosity decreasing exponentially with depth was treated. It is shown that the hodograph of the currents has a stronger curvature near the surface for eddy viscosity decreasing downwards than the ordinary Ekman spiral for a constant eddy viscosity. In Appendix II, the study of three-dimensional structure of wind waves was reviewed. A hydrodynamic model of a stationary cellular convection superposed on a horizontal current was discussed.

I. INTRODUCTION

A series of experiments on diffusion of dye patches were made by a group of oceanographers of Lamont Geological Observatory in various parts of the ocean including New York Bight and Bahama Banks (Costin and others, 1963). Among many interesting features of dye patterns which were observed in these experiments, curvature and striation are the most notable. In order to explain the two features, a more or less consistent theory is yet to be found, although the curved pattern is attributed to the Ekman type spiral (Gerard and Katz, 1963) and the striation is assumed to be caused either by shearing instability or by Langmuir streaks (Ichiye and others, 1964).

The experiment described here was planned to get more information on mechanism of curvature and striation of dye patches by choosing an experimental area off Long Island, as indicated in Fig. 1, which is relatively deep (about 55m), flat and sufficiently remote from the coast, unlike the areas where the previous experiments were made. The experimental procedure included releasing ten gallons of Rhodamine B dye solution, tracking the dye patch with a shipborne Turner Model III flurometer and taking pictures from an airplane (Costin and others, 1963). The dye solution was pumped into the water through three holes opened at the surface, 3m and 7m on a polyethylene tube which was suspended downward from the boat. Owing to some difficulties of mooring, no current meter was utilized to determine vertical structure of the current. The surface drift of the dye patches were measured by a Decca navigator system. Vertical distributions of temperature and salinity on the spot

were measured several times with a portable salinometer. Winds were measured frequently with a hand anemometer on the upper deck of the ship and also smoke signals were used occasionally to indicate the direction of wind.

The research vessel used in this experiment was R/V Kyma of New York University. The ship proceeded to the experimental area on the 10th of September, 1963 and the dye dumpings were made on the 11th and 12th, respectively. The plane used for aerial photography was a Grumman Mallarad on the 11th and a U.S. Navy C-47 on the 12th.

II. Meteorological and Hydrographical Conditions during the Experiment

The weather during the 10th and 11th of September, 1963 was rather mild. Typical weather charts of the survey period are shown in Fig. 2. The cold front passed the New York area at about 0500 of September 10. The state of the sea over the experimental area was calm from noon to about 1600 and swells of 1/2 meter high and 50 meters long came from the southeast. At about 1630 the southeast wind reached 2 Beaufort scale. On September 11th the area was covered by a high pressure area and generally the winds were moderate. The wind speed and direction measured on board the ship are listed in Table 1. The directions of wind waves were almost the same as the wind and their heights were about 0.7 meters throughout the day. However, the swells coming from the south superposed on the wind waves and thus caused cross seas after the shift of wind direction from east to south.

During the night of September 11th the southerly wind increased its speed. During the day of the 12th the wind reached 25 to 40 knots. Both wind waves and swells came from south and their height reached about

four meters in the afternoon. These strong southerly winds were caused by a cold front approaching from the west.

Table 1 Wind Measurements

Date	Time	Wind Speed (kt.)	Wind Direction
Sept. 11	0845	18	E
	1140	12	ESE
	1325	12	E
	1415	11	ESE
	1445	14	SE
	1645	12	S
	1750	10	S
	1855	12	SSE
Sept. 12	0620	16 ~ 19	SSE
	0945	18 ~ 21	SSE
	1040	20 ~ 23	SSE
	1130	22 ~ 25	S
	1155	23 ~ 26	S
	1415	35 ~ 40	S

Temperature and salinity profiles obtained with a portable salinometer are plotted in Fig. 3. It is noted that the thermocline existed below 25 meters on both days but temperature jump at the thermocline diminished conspicuously on the 12th owing to warming of deep water due to the wind stirring. Salinity distributions indicate that there was the halocline at the same depth as the thermocline on the 11th but it disappeared on the 12th.

III. Patterns of Dye Patches

Aerial photographs of dye patches were taken at several minutes' interval with a polaroid or a Graflex camera using Kodak Wratten 23A filters. Most pictures contain not only a dye patch but also the ship, so that the dimension of dye patch may be estimated. Also, the heading of the ship was recorded almost every minute and the orientation of the patch can be determined with reasonable accuracy. Several pictures contain the smoke signal released aboard the ship and the relationships

between wind and dye patch orientation were determined. Sketches of the dye patches based on aerial photographs are shown in Fig. 4. On the 11th, dye was dumped at 1000 E.S.T. This patch is called the first patch hereafter. Striations became visible about twenty minutes after the dumping. The wind direction was east or east-southeast during the time of aerial reconaissance. The striations were almost parallel to the wind direction, along which the furrows of short-crested waves were aligned. At 1040 the elongation of the patch became obvious and the striation became more regular. At 1050 the patch showed a clockwise curvature from head to tail. (At the head, concentration is high, while at the tail, the concentration is low). After 11:30 the patterns of the patch became almost stable although the size increased as the time proceeded. The curvature became striking. The striations, were in the east-west direction, almost parallel to the wind and had rather regular spacings of 50 to 100 meters. Until about 1200, the head was broad and the tail was narrow but after then, the tail became broader than head and the size of the patch increased rapidly.

On the 12th the dye was dumped at 0940 E.S.T. This patch is called the second patch. Striations began to form almost ten minutes after the dumping, earlier than on the previous day. At 1015 the striations became very conspicuous and their orientation was north-south, with spacings of 20 to 50 meters. This orientation was also almost parallel to the prevailing wind. At the same time, the whole dye patch began to elongate in the direction slightly oblique to the wind. This elongation became more and more conspicuous and its direction was deviated to the right of the wind, with angles between 20 and 30

Fig 1-A

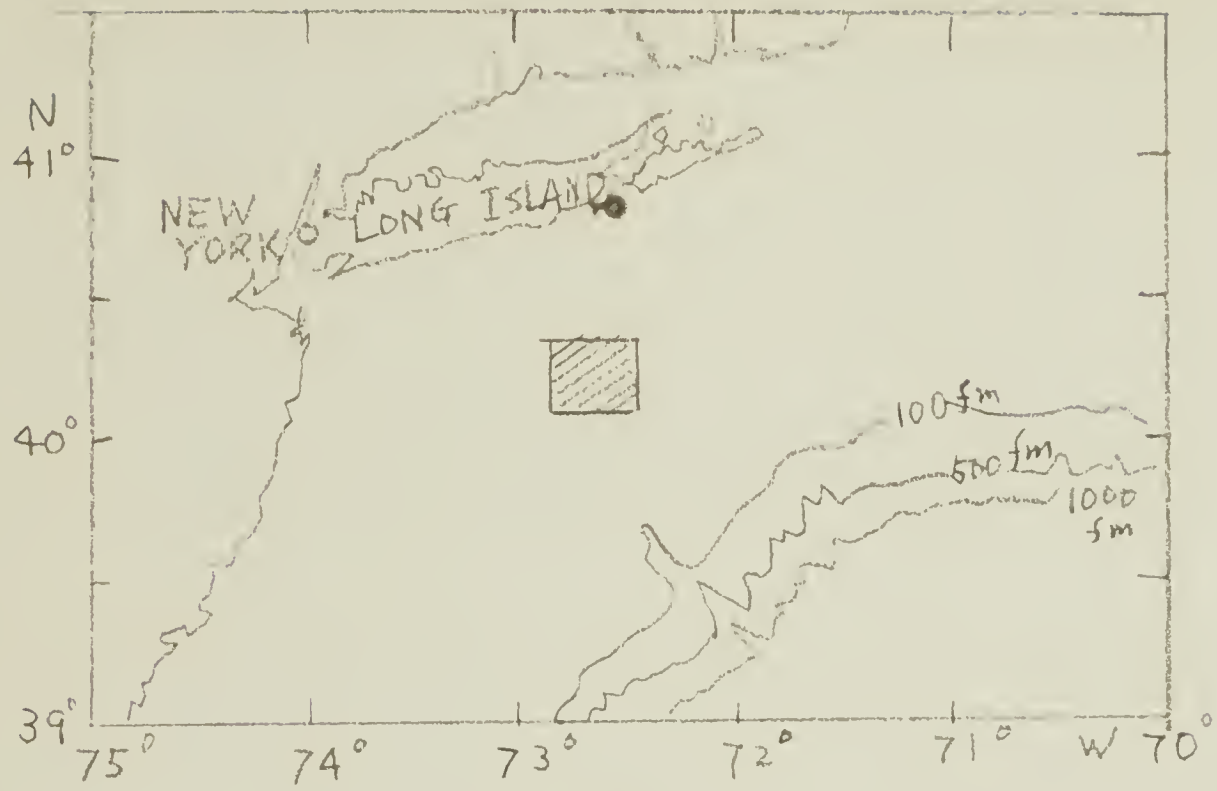
N
41°
40°
39°
NEW YORK
LONG ISLAND
100 fm
500 fm
1000 fm
75°
74°
73°
72°
71°
W 70°

Fig. 1-B

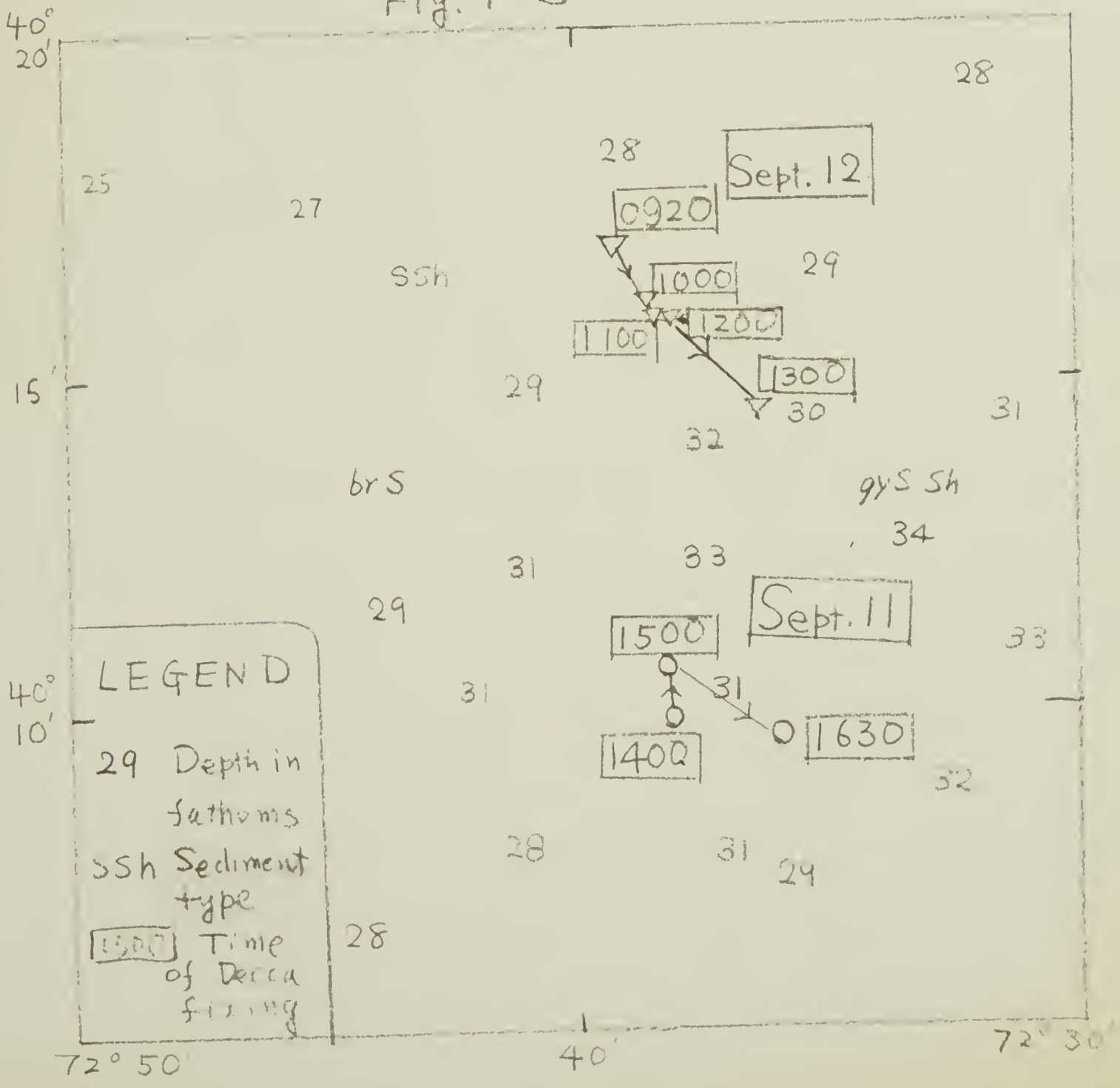
40° 20'
28
25
27
SSh
28
Sept. 12
0920
1000
29
1100
1200
1300
29
30
31
32
15'
brS
gyS Sh
34
31
33
29
Sept. 11
1500
33
40° 10'
31
31
1400
1630
32
28
31
24
28
LEGEND
29 Depth in fathoms
SSh Sediment type
1500 Time of Decca fixing
72° 50'
40'
72° 30'

Fig. 2

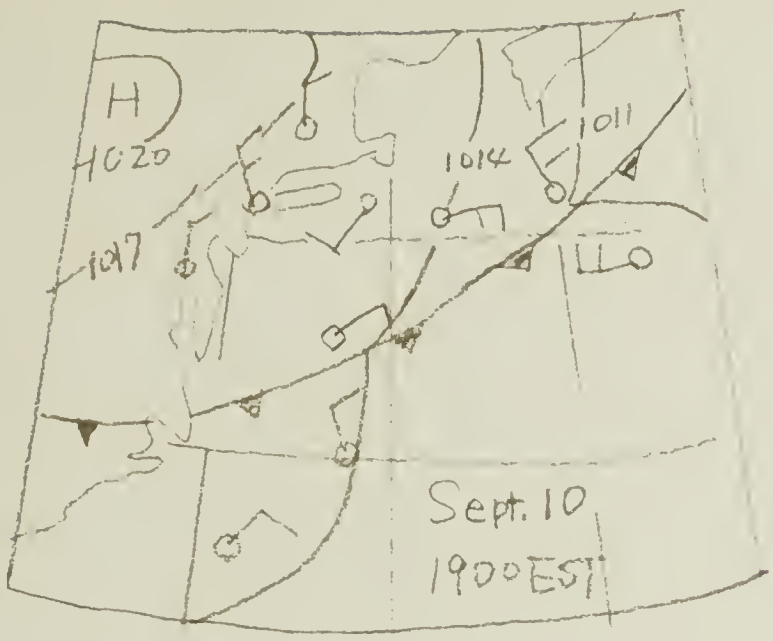
H
1020
1014
1011
1017
L
Sept. 10
1900 EST

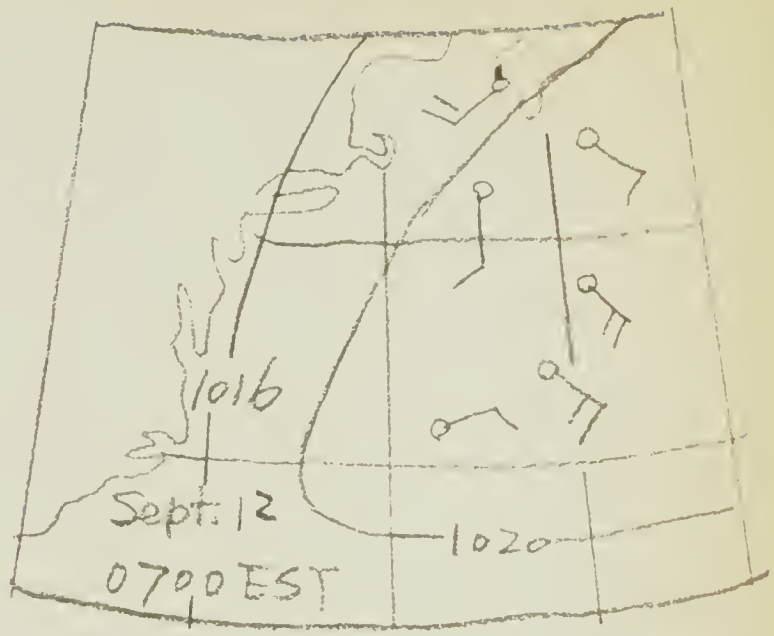
1016
Sept. 12
1020
0700 EST

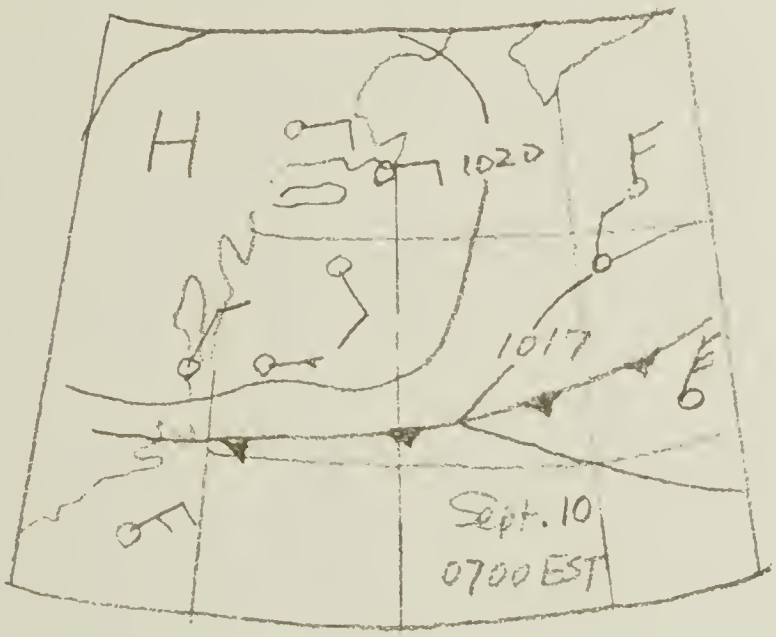
H
1020
F
1017
Sept. 10
0700 EST

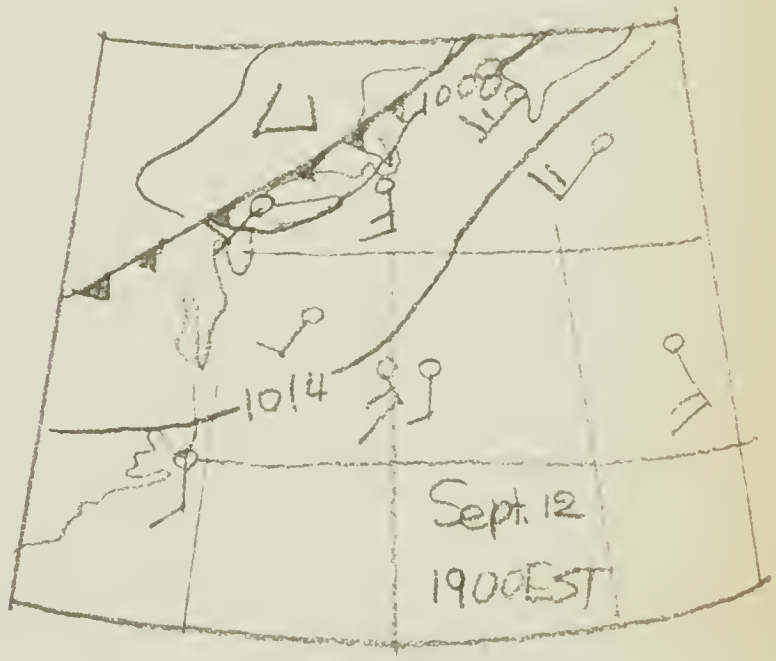
L
1000
1014
Sept. 12
1900 EST

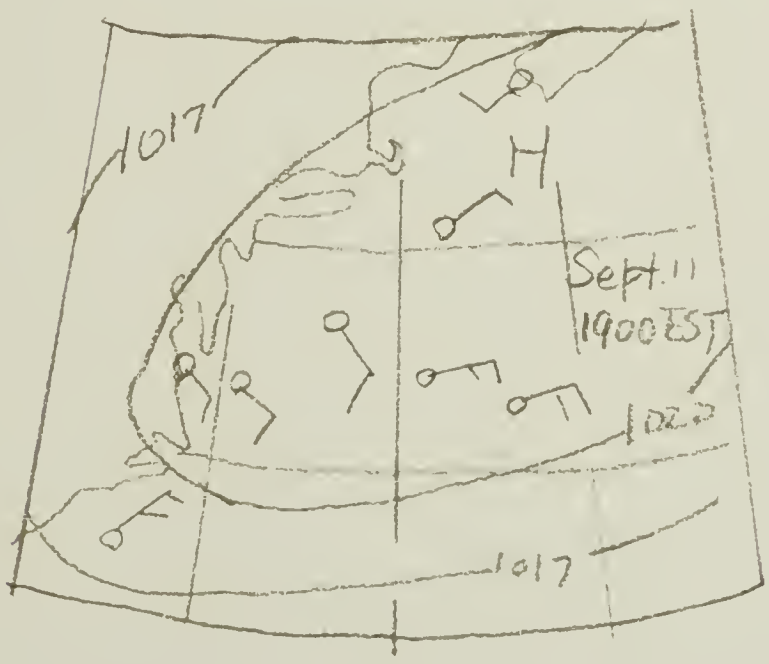
1017
H
Sept. 11
1900 EST
1023
1017

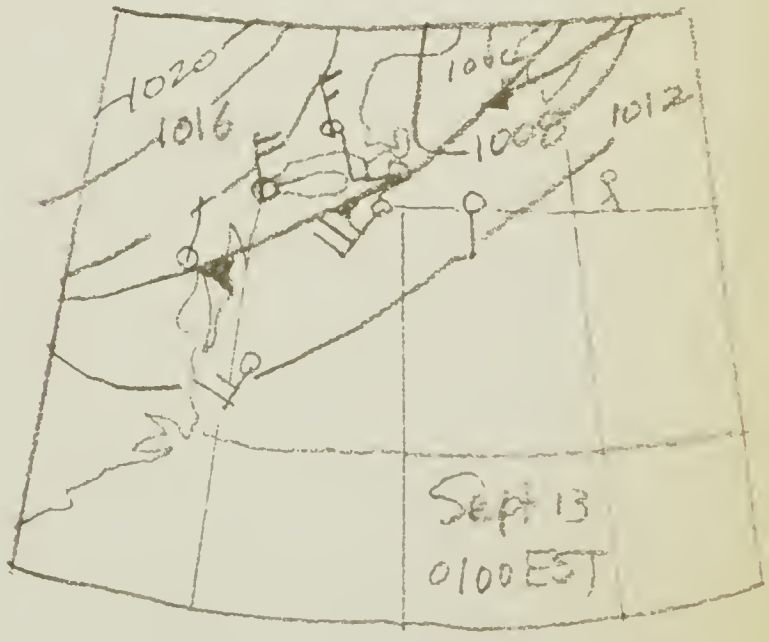
1020
1016
1004
1008
1012
Sept. 13
0100 EST

FIG. 3

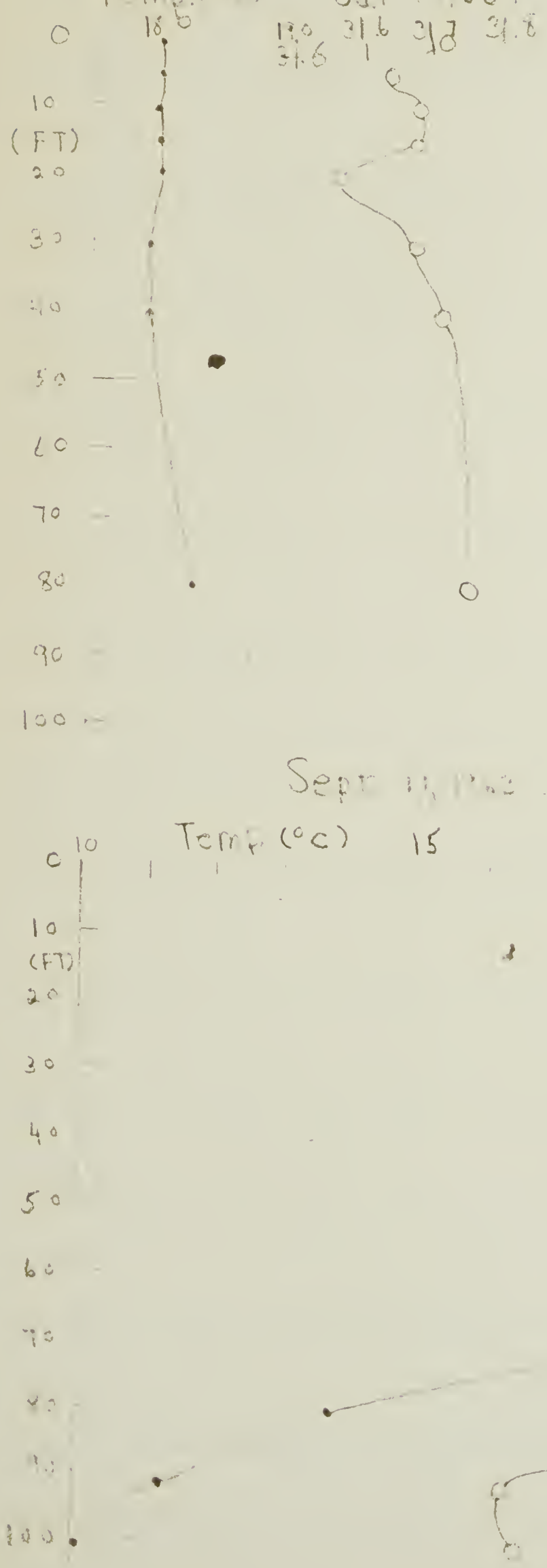
Sept 6, 1962 1200 EST
Temp. (°C)
Sal (o/oo)
18.6
19.0 31.6 31.8 31.8
31.6
0
10
(FT)
20
30
40
50
60
70
80
90
100

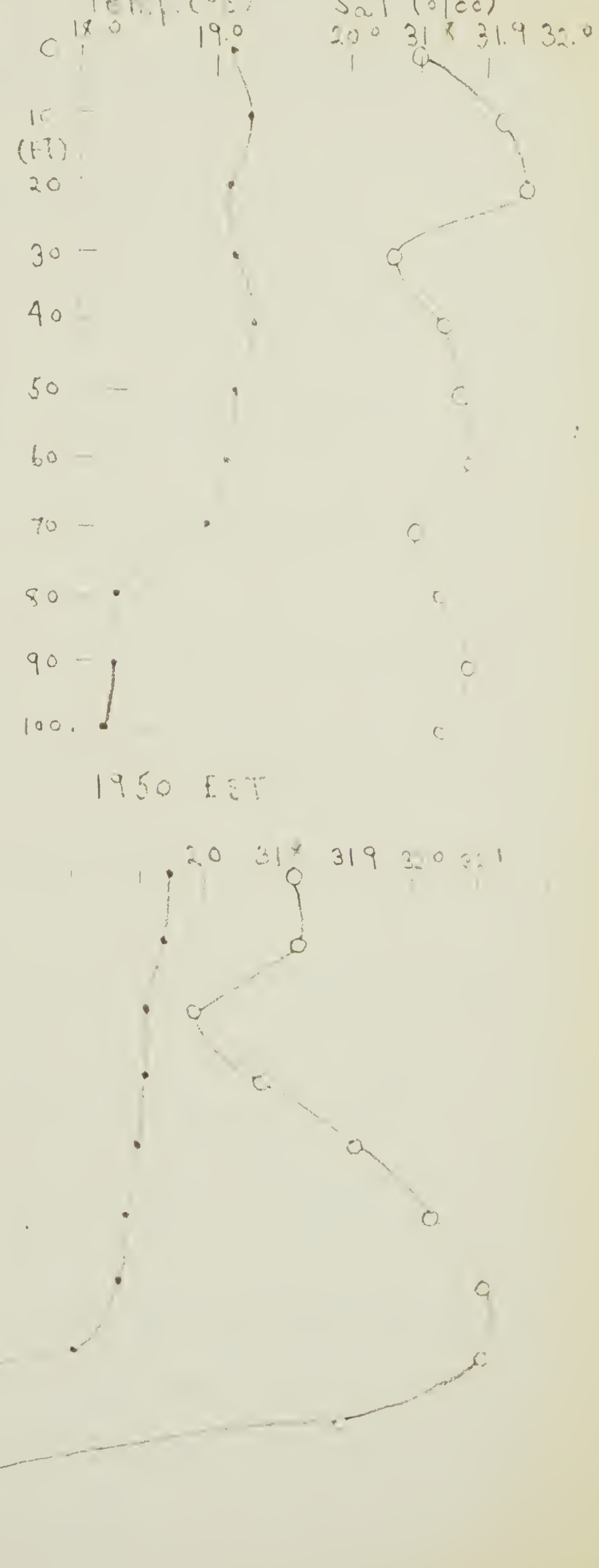
Sept. 6, 1962 1200 EST
Temp. (°C)
Sal (o/oo)
18.0
19.0
20.0 31.8 31.9 32.0
0
10
(FT)
20
30
40
50
60
70
80
90
100

Sept 11, 1962 1950 EST
Temp (°C) 15
10
0
10
(FT)
20
30
40
50
60
70
80
90
100

degrees. At about 1050 larger striations with spacings of 100 meters or more began to develop. After 1130 the pattern of the patch became rather stable except some development of larger striations. The size also gradually increased but the increase was not so conspicuous as on the previous day.

IV Vertical profiles of concentration and drift of the patches

The profiles of concentration of dye measured with the fluorometer are plotted in Fig. 5. Since no buoy system was available, such measurements were made only at head, middle and tail of the dye patches. This figure clearly indicates that the dye on the 11th spread only above 10 m but on the 12th 23 m or deeper. Also, in the first patch the dye reached almost the same depth from head to tail (axis determined from the first moment of the concentration about the depth is 3.0m, 3.1m and 3.7m at the head, the middle part and the tail respectively), but in the second patch the head seemed to reach deeper than the tail. Location of dye patches determined with a Decca navigation system is plotted in Fig. 1. On the second day, the drift of the dye patch was to the southeast between 0900 and 1300 opposite the direction of the wind. This movement seems to be due to the tidal current. The tides at Shinnecock Inlet (40°50' N, 72°28', south side of Long Island) on September 12 is as follows: HW, 0137; LW, 0800; HW, 1427; LW, 2053. The southward flow seems to correspond to the flood tide. There is no data of tidal currents in this area and it is hard to confirm the relationships between the tide and tidal currents. However, since the tidal currents are almost uniform vertically except close to the bottom, their effect is to transport the entire part of the dye patch.

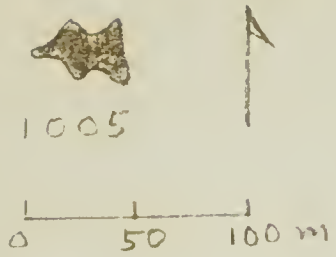

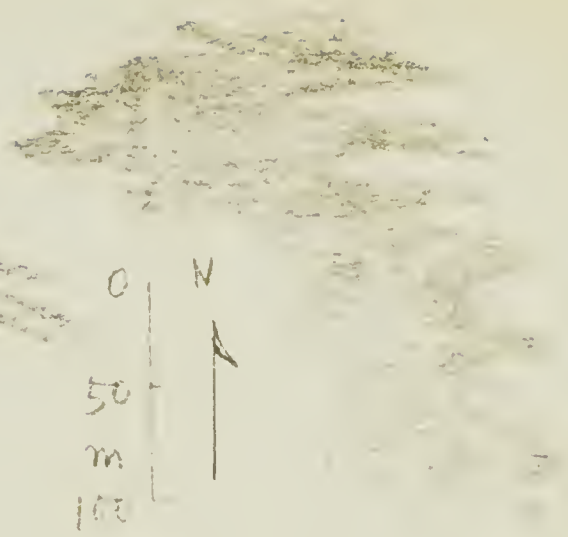

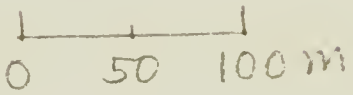

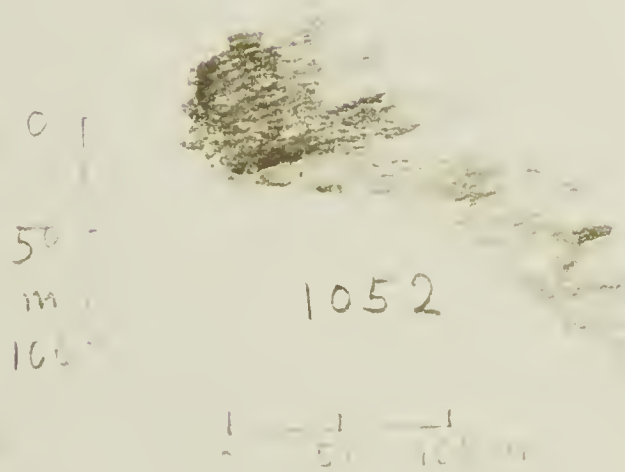

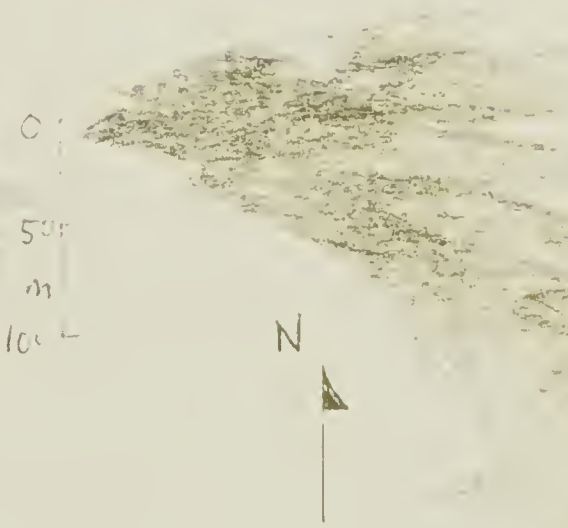

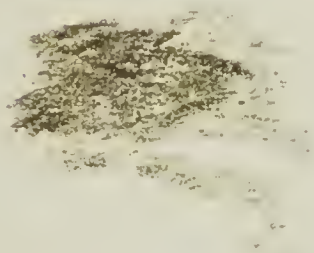

Sept. 11
1963
FIG 4-A

N

0 . 100 m

1122

SMOKE

N

0

100

200

1147

1127

0 100 200 m

(1150)

0 100 200m

(1139)

N

1157

N

1137

WIND
(12 KT)

Sept. 11

1963

FIG. 4-B

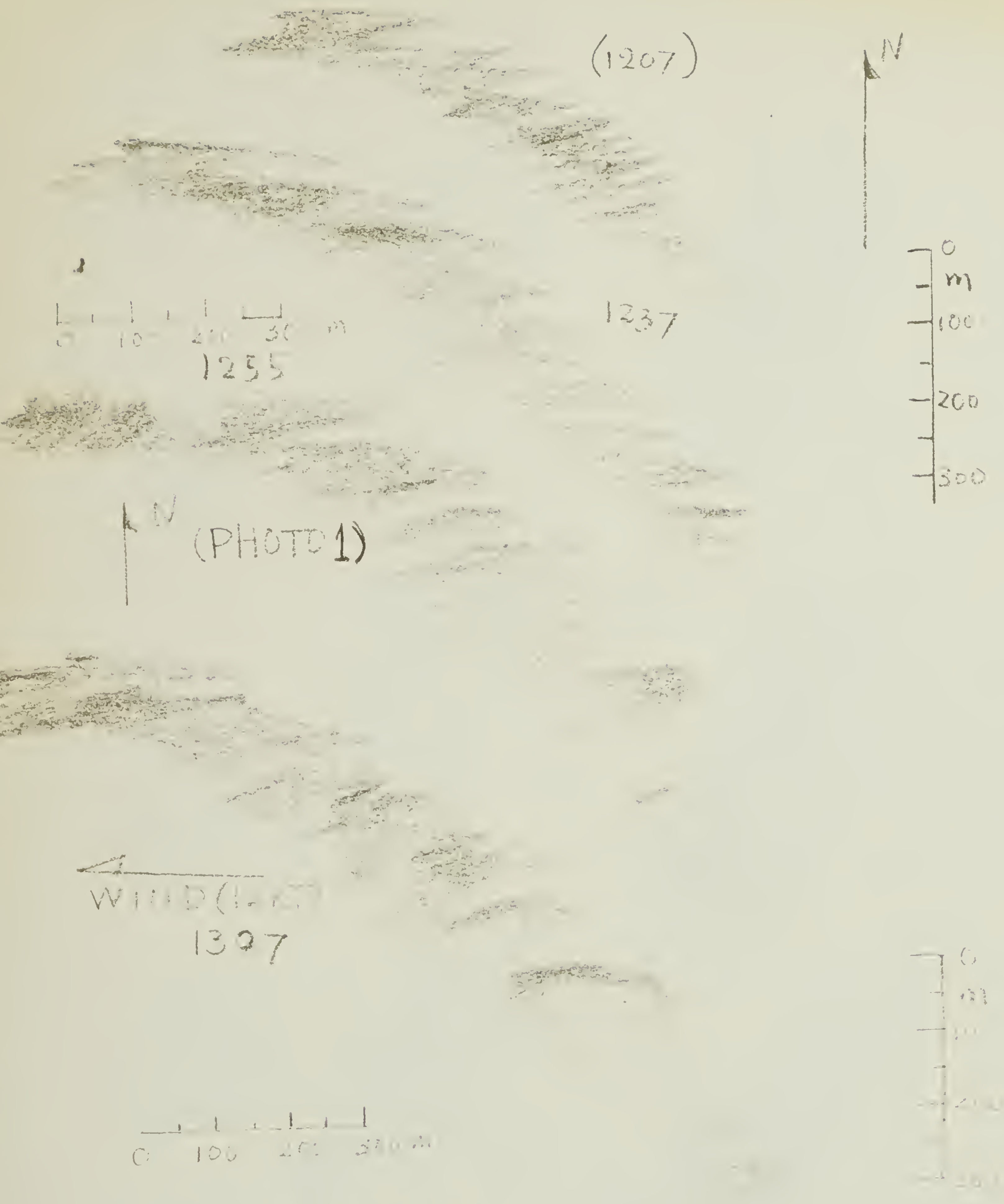

Sept. 11 1946

FIG 4-C

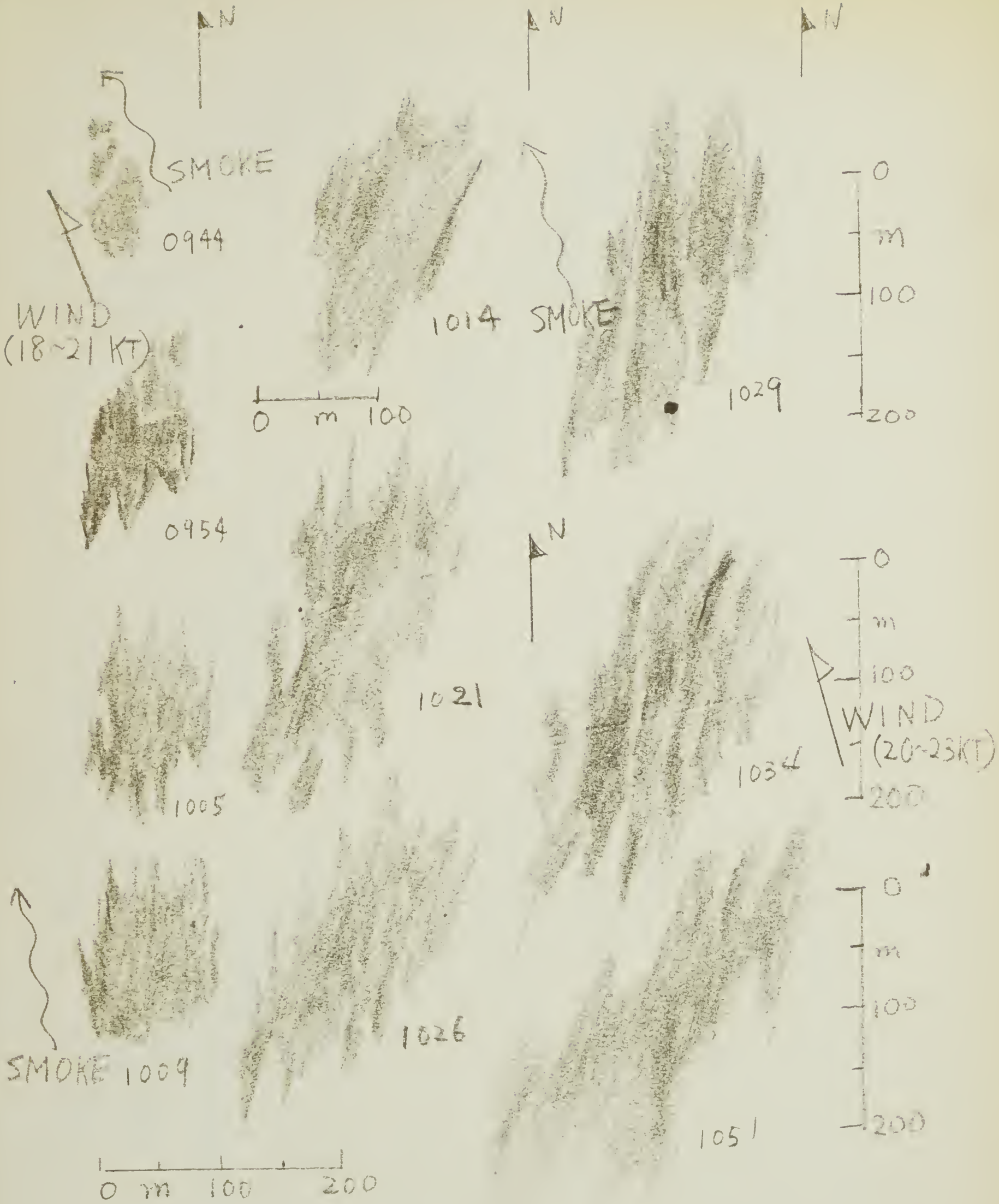

Sept. 12, 1963

FIG. 4-D

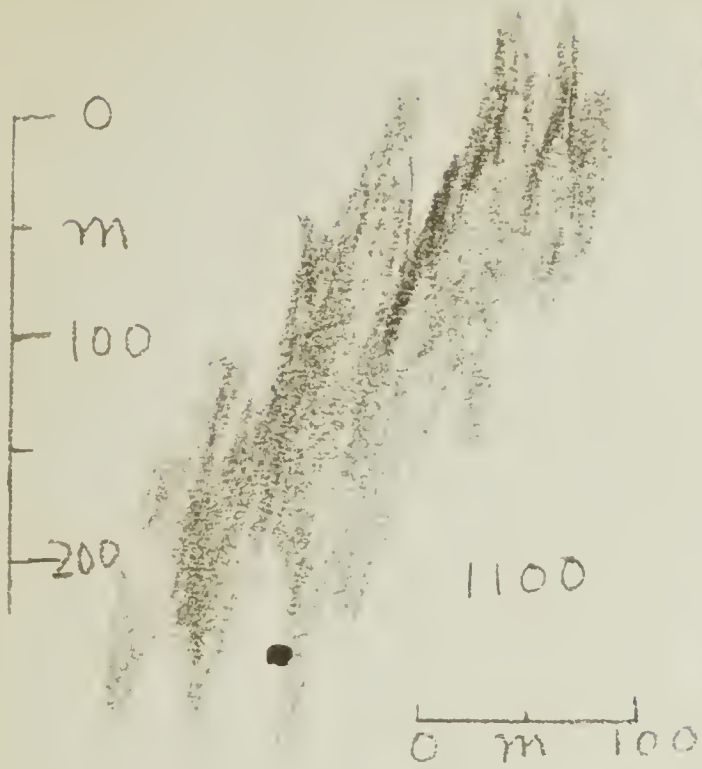

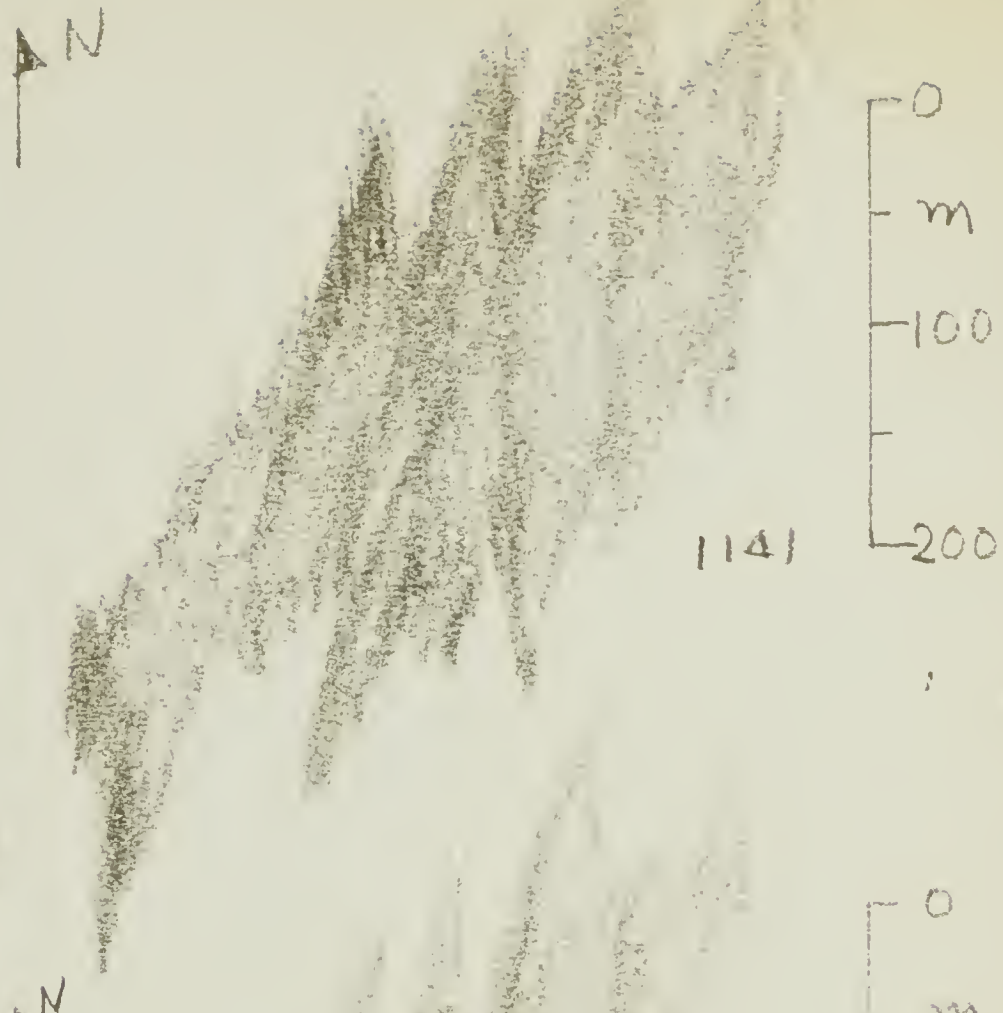

0 m 100

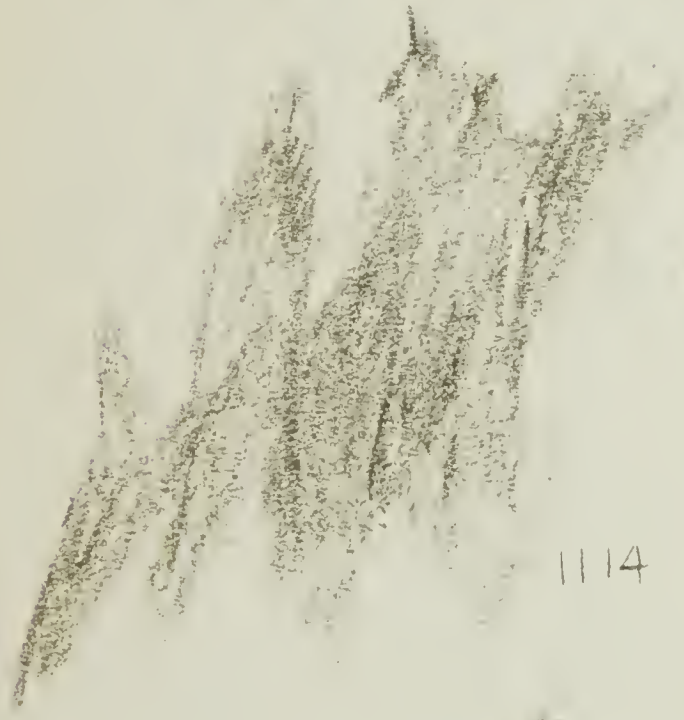

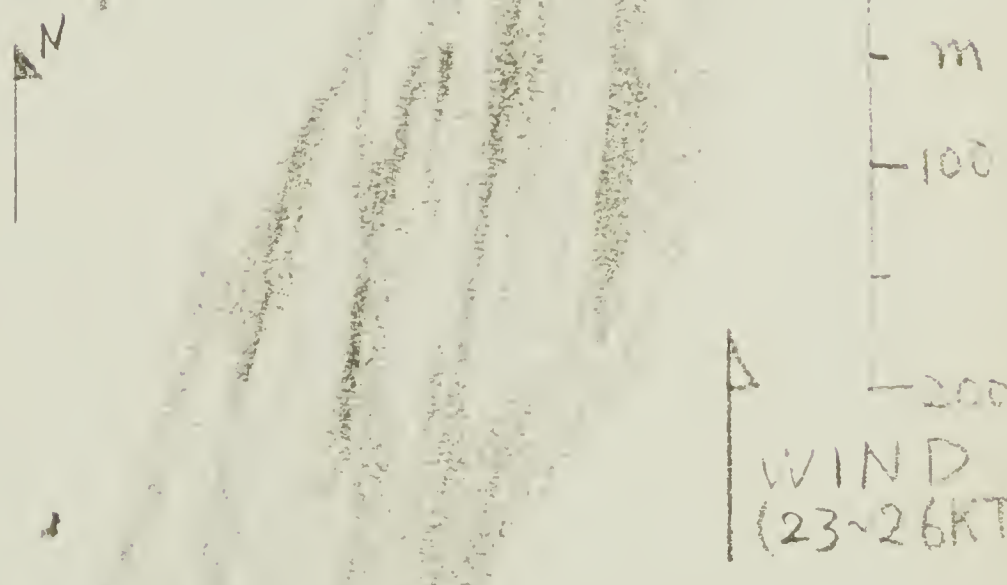

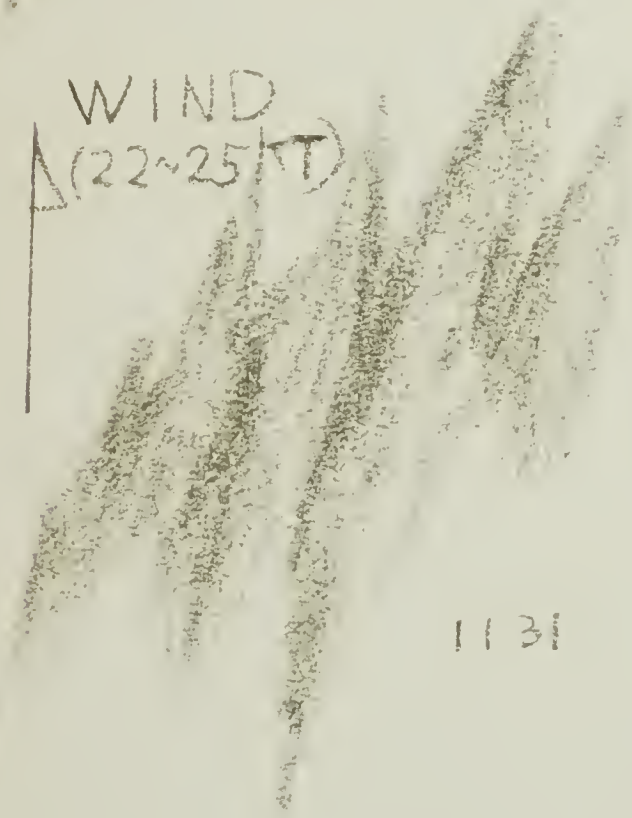

0 m 100

Sept. 12, 1963

FIG. 4-E

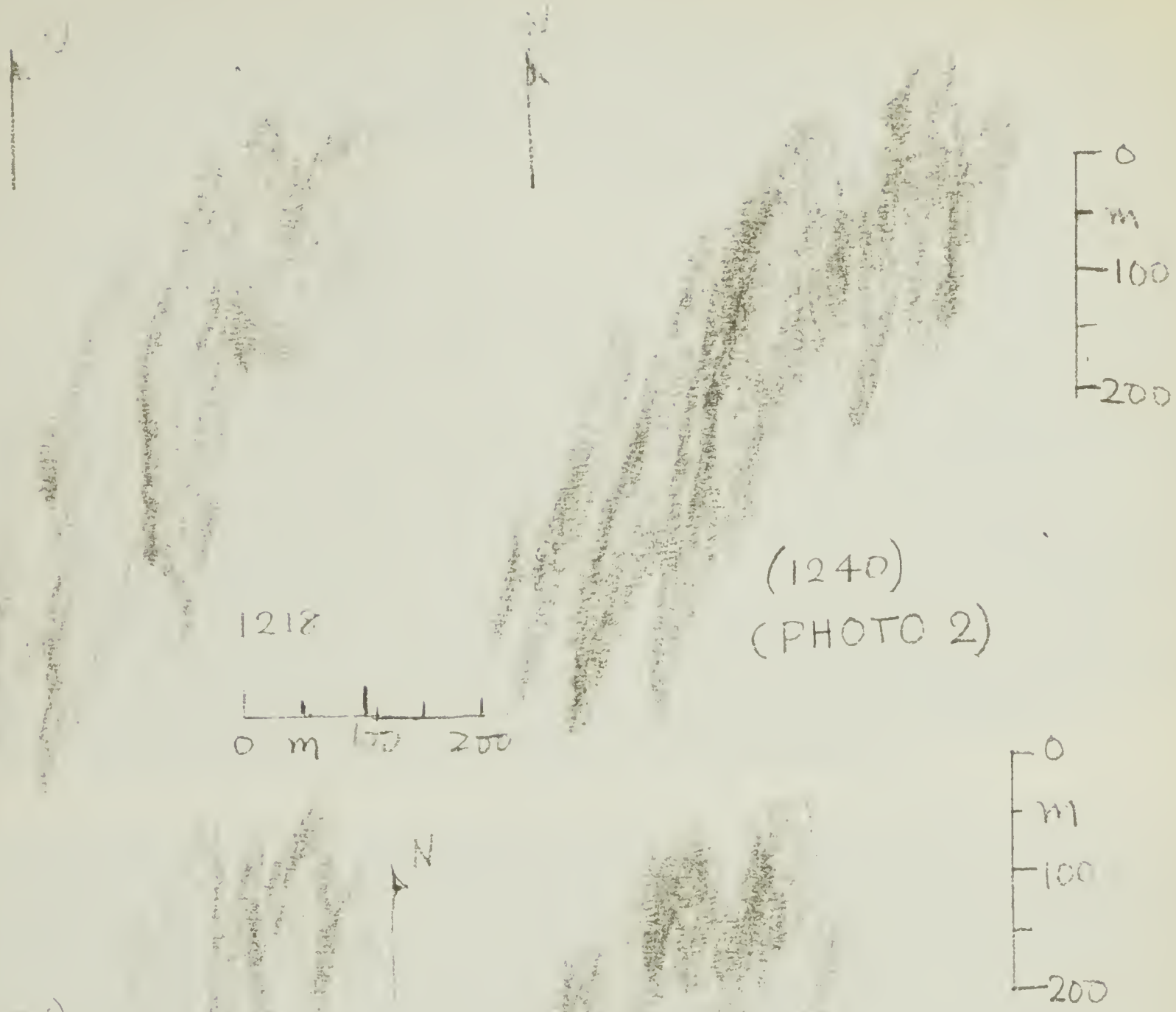

Sept 12, 1963

Fig. 4 F

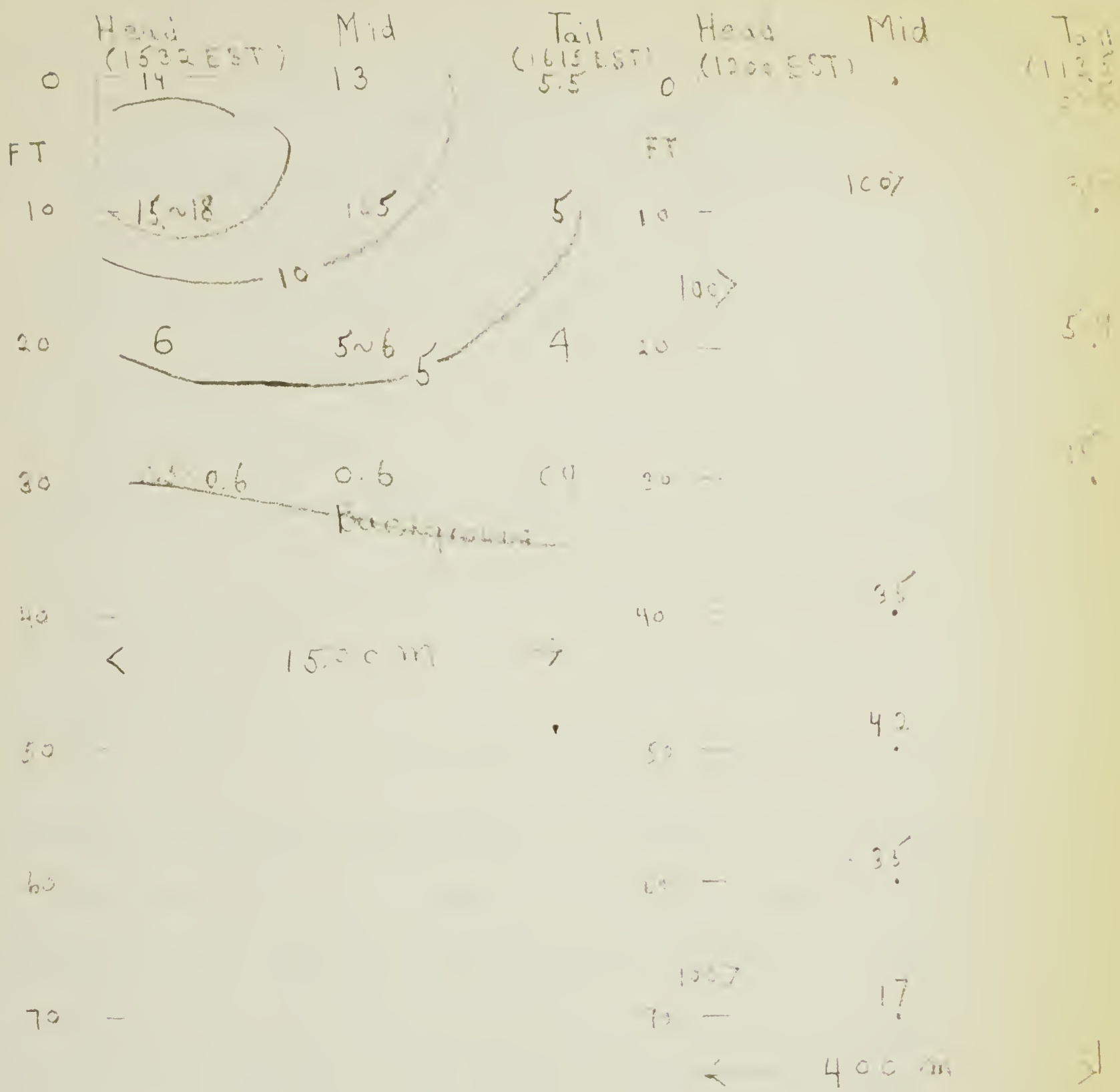

FIG 5 O$_3$ concentration in ppb.

Therefore, in the present experiment dealing with a moving source, the pattern of the dye patch might not be disturbed by presence of tidal currents.

In Fig. 4 the directions of smoke and wind direction and speed measured with a hand anemometer were inserted whenever such data were available. Also, the time indicated with parenthesis means that a photograph at that time did not show the ship and thus the size of the patch was estimated by interpolation.

Photograph 1 shows the first patch at 1255 on September 11th and Photograph 2 shows the second patch at 1240 on the 12th. The altitude at which the pictures were taken was 1300 m for the first patch and 650 m for the second patch.

V Theoretical Discussions

One of the striking features of the dye patches at this experiment is that the first patch showed a conspicuous curved tail, while the second patch elongated but was rather straight. The vertical distributions of dye concentration in Fig. 5 indicate that dye was found only above 10 meters in the first patch but it penetrated deeper than 20 m in the second patch suggesting that the vertical mixing was more intense on the second day owing to the stirring effect of winds. The warming of water below the thermocline on the second day (Fig. 3) indicates that the effect of stirring reached below the thermocline.

The lack of curvature in the second patch may be due to the increase of the vertical eddy viscosity by the effect of wind stirring. The depth of frictional resistance D for a constant eddy viscosity equals to $(2\nu/f)^{\frac{1}{2}}$ where ν is the eddy viscosity and f is the Coriolis' parameter.

(Sverdrup et al, The Oceans, pp. 492-493). When the eddy viscosity increases, D also increases. If D becomes larger than the depth of the sea, the Ekman spiral does not develop and instead the velocity vector tends to have almost the same direction throughout the depths, although the directions are reversd near the bottom (Defant, 1961, p. 402). This prediction based on the classical Ekman theory of the wind current in the sea of a finite depth can be applied to the second patch. It was elongated to the direction deviated clockwise by about 20 to 30 degrees from the wind and there was no curvature.

The curvature of the first dye patch, which was clearly recognized almost one hour after the dumping, seemed to be due to the Ekman spiral, when the eddy viscosity and thus the friction depth D are sufficiently small, so that the effect of the bottom did not influence the structure of the wind current. In fact, the wind of 8 to 12 knots was almost constantly blowing from east southeast or east since the afternoon of the 10th of September. Owing to the moderate wind, the eddy viscosity was not so large as in the second patch and thus the Ekman type wind currents were well established during the morning of the 11th. This is the reason why the curvature of the dye patch so quickly developed.

When the eddy viscosity decreased rapidly with depth, the curvature of the hodograph of the Ekman spiral becomes larger than for the uniform eddy viscosity, particularly near the surface (Fjeldstat, 1929). The eddy diffusivity decreasing with depth also makes vertical diffusion of dye concentrate near the surface as manifested by the first patch. The analytical discussion on the drift current due to the

eddy viscosity variable with depth is presented in Appendix 1.

The patterns of dye patches described in Fig. 4 indicate conspicuous striations which were almost parallel to the wind direction on the second day. On the first day, the striations were parallel to the wind which was easterly at first, but after the wind shifted to the south, reorientation of the striations did not immediately follow.

The orientation of striations suggest that it might be caused by surface streaks which were explained as the effect of surface film by Welander (1962). However, the wide spacings (a few hundred meters) and slow response of alignment to wind directions are quite contrary to the conditions envisaged by Welander.

The process of development of striations will be described in the following, according to visual observations on board the ship and inspection of aerial photographs. On September 11th, wind waves came from east in the morning due to the easterly wind as described in Section 2. Aerial photographs at 1022, 1040 and 1127 indicate that the furrows or streaks with a width of about a ship's length (22 meters) were superposed on this wave pattern, ran from east to west and were orthogonal to the crest lines of waves which have crest lengths of three to four ships' length. No definite meteorological disturbance which might generate such swells is seen in weather charts of Fig. 2. Also, these furrows or streaks appeared to be almost stationary. Close inspection of the photographs mentioned above shows that the furrows seem to correspond to the dark bands between the striations. This suggests that the furrows were associated with the divergence or convergence of the surface current.

On the 12th, striation began to develop almost 20 minutes after the dumping. Although the furrows parallel to the wind were recognized, they were not so clear as on the previous day. The spacings of striations were irregular and smaller than a ship's length at first. The striations were developed leeward in the subsurface part of the dye patch as seen from the direction of smoke contrary to the case of the previous day. Fingers of the dye patch seemed to be elongated in the direction of currents produced by breaking of wave crests. After 40 to 50 minutes of the dumping, the fingers developed windward and spacings reached several ships' length. In this stage, the direction of elongation of the whole patch was deviated to the right of wind direction as stated in Section 3, but the striations were oriented almost parallel to the wind.

It is quite certain that the three dimensional structure of waves or short-crested waves are important to the generation of striations. As Phillips (1957) and Lighthill (1962) discussed, turbulence of wind may be an important factor to wind waves in the developing stage. As explained in Appendix II, shorter waves including capillary wave regime propagate statistically in two main directions with angles more than 60° to the mean wind direction. The interference among these wave trains seems to produce alternatively rough surfaces along the crests whose width is more than several wave lengths and smooth surfaces along the furrows which are aligned with the mean wind directions. The differential roughness along the (short) crests and along the furrows is twofold. The large roughness along the crests causes increase of the shear in the surface layer of the water and thus faster surface currents than along the furrows, occasionally reinforced by breakings of tips of

waves. This produces fingers of the dye patch. Also, the reduced shear along the furrows due to the smooth surface causes the divergence or convergence of the surface current there (Appendix II). Along the divergence line, the water with less concentration of dye is brought from below to the surface, thus forming the dark bands between the striations.

ACKNOWLEDGMENT

The field work, on which this study is based, was carried out with help of M. Costin, N. Plutchak and a crew of the KYMA, New York University Research vessel. The aerial photographs were taken by B. Katz who also was helpful in interpreting these photographs. The assistance of these people, including R. Gerard who gave some suggestions on the manuscript is gratefully acknowledged. The author also wishes to express his gratitude to Dr. W. Pierson of New York University for his permission to use the KYMA and to R. Stevens of the Office of Naval Research for coordination in planning the field work. Special thanks are due to Admiral H. T. Deutermann, Commander of Eastern Sea Frontier for making one of his planes available for this project and to the crew of the plane for their enthusiastic participation in the experiment.

The work reported in this paper was supported by the Atomic Energy Commission under Contract AT-30(2663) and by the Office of Naval Research under contract Nonr 266(48).

Appendix I - Wind-driven Current for an Eddy Viscosity Variable with Depth

Effects of surface waves on generation of turbulence in the water were discussed semi-empirically by Dobronklonsky (1947) and Shebalin (1957), Ichiye (1962). The heuristic result of these studies is an expression of the eddy viscosity due to waves. When the depth is finite, the eddy viscosity η is given by

$$\eta \approx \frac{\pi k_0^2 \rho \zeta^2}{3 \epsilon T} \cdot \frac{\sinh^2 2k(H-z)}{\sinh^2 kH \cosh^2 2k(H-z)} \qquad (1)$$

where k_0 is Karman's constant (=0.4), ρ the density of the water, ζ the wave height, T the period, k is the wave number, z is the depth below mean sea level and H is the depth of the water. When the water is deep compared with the wave length, this equation becomes

$$\eta \approx \frac{\pi k_0^2 \rho \zeta^2}{18 T} e^{-2kz} \qquad (2)$$

These two relations indicate that in general, the eddy viscosity increases with increasing height and frequency and that the ratio of its decrement with depth becomes larger as increasing wave number.

In order to examine dependence of the Ekman wind current on differences of the eddy viscosity, the simple case of steady state and pure drift current is treated. Also, for mathematical simplicity, the eddy viscosity of the type of equation (2) is assumed, though the depth is taken finite. The equations of motion are given by

$$i f \bar{W} = \frac{d}{dz}\left(\eta_0 e^{-\alpha z} \frac{d\bar{W}}{dz}\right) \qquad (3)$$

where $W = u + iv$, u and v being x- and y- components of current, respectively. The boundary conditions at the surface (z = 0) and at the bottom (z = h) are expressed by

$$-\eta_0 \frac{d\bar{W}}{dz} = i\tau \qquad (4)$$

$$\overline{W} = 0 \tag{5}$$

in which the wind stress τ is assumed to have y- component only.

When the variable (z) is changed into x, using the relationship

$$x = e^{-\alpha z} \tag{6}$$

equation (3) becomes

$$x \frac{d}{dx}\left(x^2 \frac{d\overline{W}}{dx}\right) = i\beta^2 \overline{W} \tag{7}$$

where $\beta^2 = \epsilon/(\eta_0 \alpha^2)^{-1}$. The boundary condition (4) is rewritten as

$$\frac{d\overline{W}}{dx} = iT \qquad (at \quad x = 1) \tag{8}$$

where $T = \tau (\alpha \eta_0)^{-1}$. The solution of equation (6) can be expressed by cylinder functions like

$$\overline{W} = x^{-\frac{1}{2}} \left\{ A H_1^{(1)}(\beta x^{-\frac{1}{2}}) + B H_1^{(2)}(\beta x^{-\frac{1}{2}}) \right\} \tag{9}$$

where $\beta = \sqrt{2}/\alpha(1-\gamma)$ and $H_1^{(1)}$ and $H_1^{(2)}$ are Hankel's function of the first and the second class, respectively. Integration constants A and B can be determined from the boundary conditions at the surface (x = 1) and at the bottom [x = a = exp (-αh)]. The conditions (8) and (5) respectively lead to the following relationships:

$$A H_0^{(1)}(\beta) + B H_0^{(2)}(\beta) = -2T\beta^{-1} i \tag{10}$$

$$A H_1^{(1)}(\beta a^{-\frac{1}{2}}) + B H_1^{(2)}(\beta a^{-\frac{1}{2}}) = 0 \tag{11}$$

Substitution of the values of A and B determined from (10) and (11) and (9) yields

$$W = \frac{-2T\beta^{-1} i \exp(\frac{1}{2}\alpha z)}{m_1 n_2 - m_2 n_1} \left\{ n_2 H_1^{(1)}(\beta e^{\frac{1}{2}\alpha z}) - n_1 H_1^{(2)}(\beta e^{\frac{1}{2}\alpha z}) \right\} \tag{12}$$

where

$$m_j = H_2^{(1)}(\beta) \; ; \; n_j = H_1^{(1)}(\beta e^{\frac{1}{2}\alpha h}) \quad , (j = 1, 2) \qquad (13a, b)$$

When αh is much less than unity, the eddy viscosity is almost uniform with depth and the solution for wind-driven currents is almost the same as the original one by Ekman. Therefore, the interesting case is that the eddy viscosity decreases rapidly with depth or the parameter αh is much larger than unity. When the depth is taken as 50 m, equation (2) yields $\eta_0 = 25 \; (cm^2/sec)$, $\alpha = 10^{-2} (cm^{-1})$ for waves with wave length 13.6 m, wave height 0.5 m and period 3 sec. With these values of η_0 and α we have

$$|\beta| = 2p = 0.08 \; ; \; |\beta| e^{\frac{1}{2}\alpha h} = 6 \times 10^{10} \qquad (14)$$

Therefore, m_j can be expressed by an expansion of Hankel function for a small value of argument while n_j is given by its asymptotic expansion. When only the first order term is retained, we have

$$m_j = (-1)^j \, i \left(\frac{2}{\pi}\right) \ln \gamma\beta \quad , (j = 1, 2) \qquad (15)$$

$$n_1 = \left(\frac{2}{\pi \pi_0}\right)^{\frac{1}{2}} \exp\left\{-\frac{5\pi}{8} i + 2^{-\frac{1}{2}} \pi_0 (1-i)\right\} \qquad (16a)$$

$$n_2 = \left(\frac{2}{\pi \pi_0}\right)^{\frac{1}{2}} \exp\left\{-\frac{7}{8}\pi i - 2^{-\frac{1}{2}} \pi_0 (1+i)\right\} \qquad (16b)$$

where $\pi_0 = 2p e^{\frac{1}{2}\alpha h}$ and γ is Euler's constant (=1.781) (Jahnke and Ende, 1945). Equations (15a) and (15b) indicate that $|n_1| \gg |n_2|$. The approximate expression for W in the depth range satisfying $\alpha z \lesssim 1$ is given by

$$\overline{W} = \frac{\alpha \tau}{2f} K e^{i\psi} \qquad (17)$$

$$K = \left\{\left(\frac{\pi}{4}\right)^2 + (\ln \gamma p)^2\right\}^{-\frac{1}{2}} \qquad (17a)$$

$$\tan \psi = \frac{\pi}{4} / \ln(1/\gamma p) \qquad (17b)$$

It is noted that the expression (17) does not depend on z explicitely. The value of ψ corresponding to p = 0.04 given by (14) equals 0.21 or about 12°. Therefore, the surface drift deviates from the wind to the right by about 78°, in contrast to the classical Ekman drift.

When the depth satisfies the relation $\alpha z \gg 1$, the approximate expression for W becomes

$$W = \frac{\tau_x}{\rho}\left(\frac{\pi}{\delta}\right)^{\frac{1}{2}} K e^{i(\psi - \frac{\pi}{4})} \left\{ \exp 2^{-\frac{1}{2}}(\pi - \pi_c)(1-i) - \exp\left[2^{-\frac{1}{2}}\pi(1-i) - \frac{\pi}{4}\right]\right\} \quad (18)$$

where $r = 2\rho e^{\frac{1}{2}\alpha z}$. The distribution of current vectors with depth for the same numerical values of π_c , k and h as leading to (14) are plotted in Fig. 6. It is remarkable that the decrement of velocity with depth is quite rapid and that the curvature of the resultant spiral is quite conspicuous near the surface. For comparison, the vertical structure of the wind-driven current for the constant eddy viscosity is shown in the curves taken from Defant (1961) in Fig. 5. In these curves, $D = \pi\left(\frac{2A}{f}\right)^{\frac{1}{2}}$ is the frictional depth and thus D equaling to 4h, 2h or 0.8h yields the eddy viscosity of 2×10^3, 5×10^2 or 80 (cm^2/sec), respectively, when h = 50 m. All these curves indicate that the curvatures of the spiral are not so strong near the surface as in the previous example.

Kozlov (1963) treated the similar problem with eddy viscosity varying with depth according to a power law like $(h - z)^n$ His result (Fig. 1 in his paper) also indicates that the curvature of the spiral becomes more conspicuous as n increases, although his curves show larger curvature towards the bottom.

Fig. 6

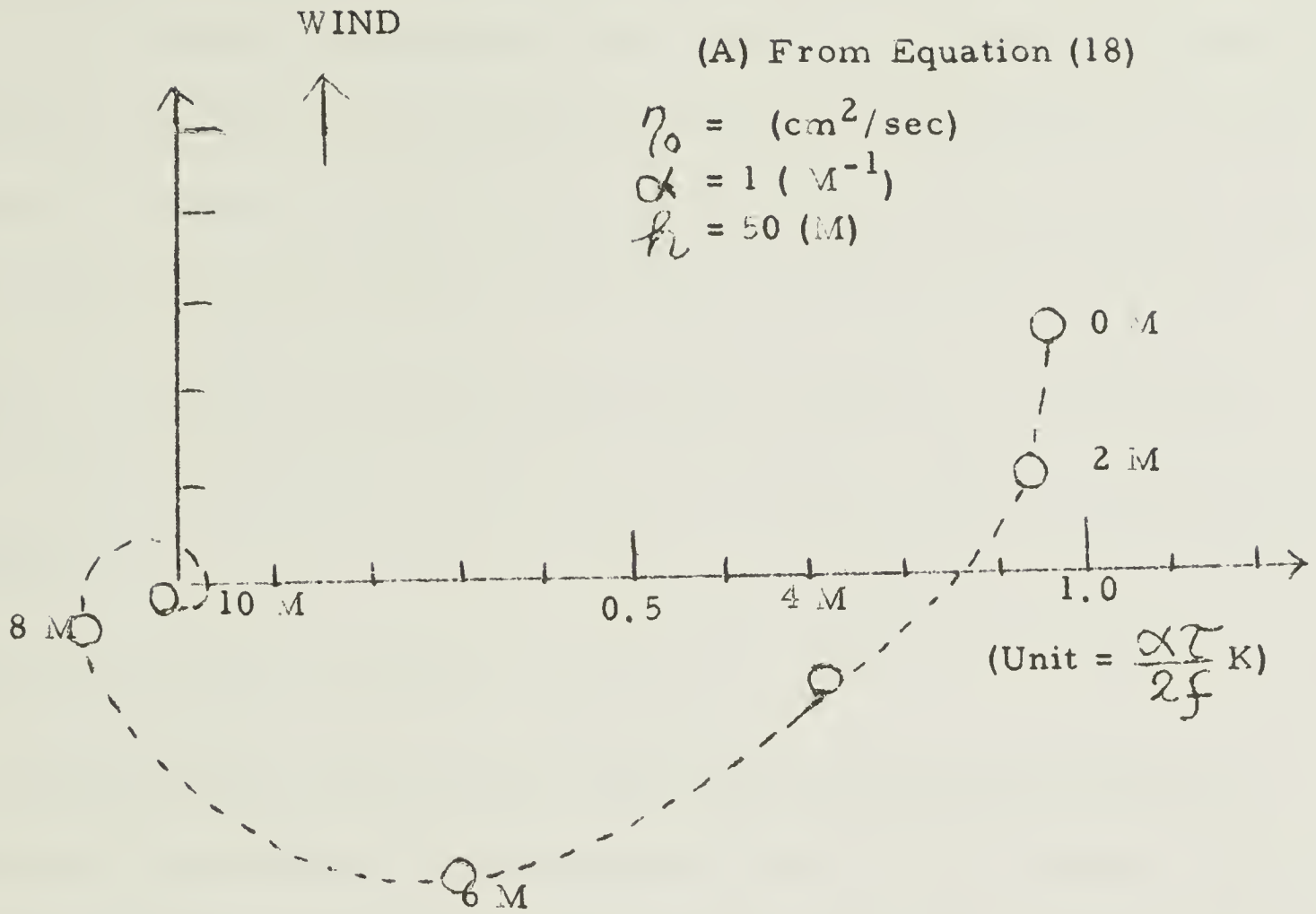
WIND
(A) From Equation (18)
η_0 = (cm²/sec)
α = 1 (M⁻¹)
h = 50 (M)
0 M
2 M
10 M
0.5
4 M
1.0
8 M
6 M
(Unit = $\frac{\alpha\tau}{2f}$ K)

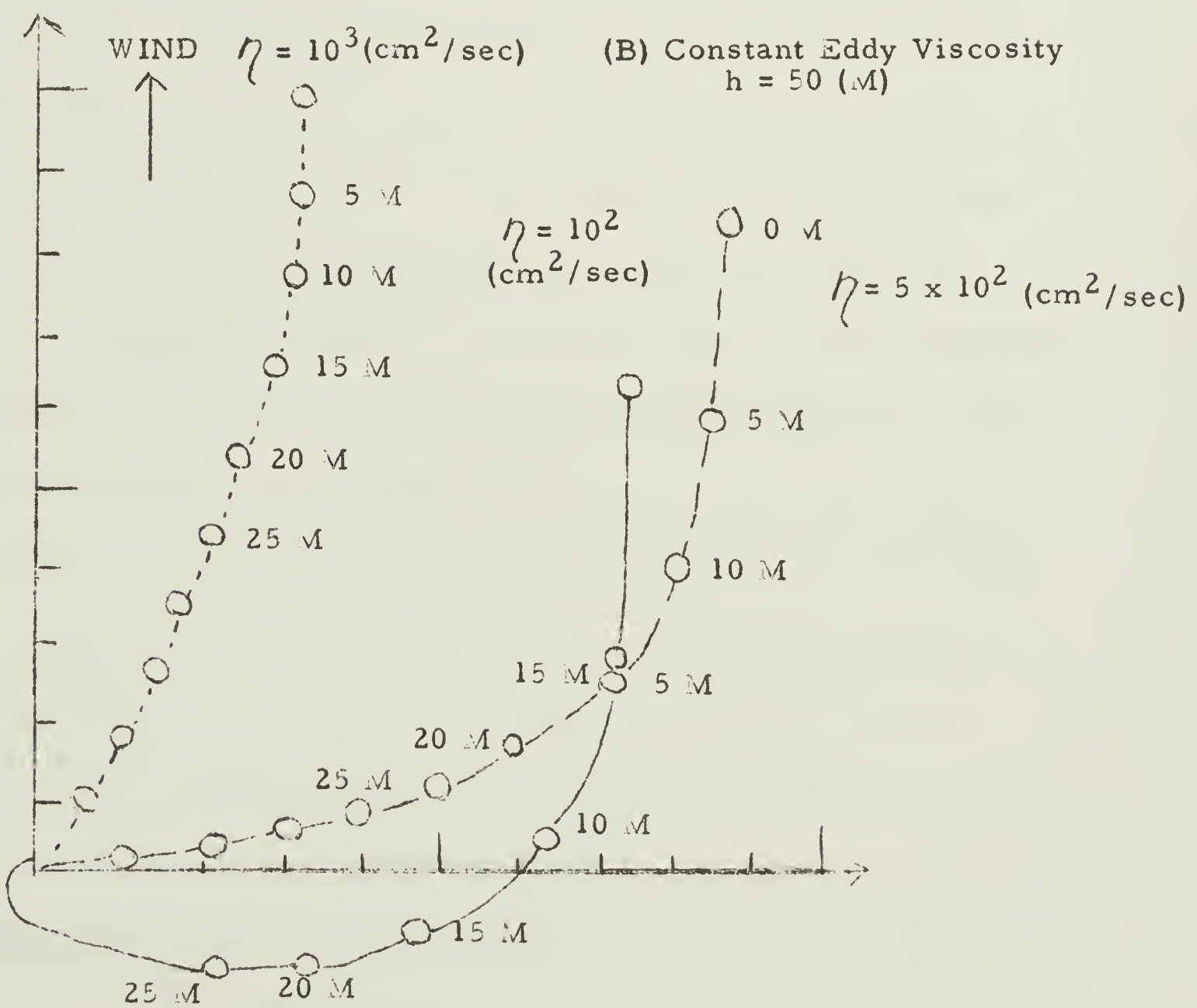
WIND
η = 10³(cm²/sec)
(B) Constant Eddy Viscosity
h = 50 (M)
5 M
10 M
15 M
20 M
25 M
η = 10² (cm²/sec)
0 M
5 M
10 M
15 M
η = 5 x 10² (cm²/sec)
20 M
25 M
10 M
15 M
25 M
20 M

Appendix II Mechanism of Striations of Dye Patches

At the present time there are two kinds of theory explaining generation of waves by wind. One is a model considered by Phillips (1957) who discussed the random pressure fluctuations associated with turbulent wind as a main cause of wind waves. His theory indicated that waves with length λ would be resonantly generated if an angle θ between their direction of propagation and that of convectional pressure pattern having a speed u satisfied

$$U \cos\theta = C$$

where C is the phase velocity (= $\sqrt{g\lambda/2\pi}$).

Another theory developed by Miles (1957) explained the growth of waves as an instability in the shearing flow of air-water system. This model is based on the purely two-dimensional structure of the mean wind which varies only in the vertical direction. The turbulence of the wind plays no essential part in this model. Later Miles (1960) combined these two models. He showed that in the initial stage of wave generation the random pressure excited the interface oscillations which are then augmented by the instability of shear flow. Longuet-Higgins (1963) showed that Miles' model is more realistic, since a turbulent component in the mean square air pressure was at least two orders of magnitude smaller than postulated in Phillips' theory. From measurements of vertical displacement and slopes of sea level with a floating buoy, he determined the directional spectrum $F(\sigma, \phi)$ of the surface waves. This directional spectrum is defined so that $F(\sigma,\phi)\,d\sigma\,d\phi$ is the contribution to the mean square value of surface displacements due to wave elements which have ranges of frequency $(\sigma, \sigma+d\sigma)$ and direction $(\phi, \phi+d\phi)$.

He then determined an approximate r.m.s. angle ψ between the direction of wave propagation and that of the wind for different values of σ . The values of ψ obtained from a measured spectrum is in good agreement with Miles' formula $\cos^{-1}(c/U_w)$, where c is the wave velocity (= $\sqrt{g\lambda/2\pi}$) and U_w is the wind velocity at a height of 0.2 wave lengths. Thus, for the waves with periods shorter than 3.3 seconds, the values of ψ are within a range of 50° to 70°, slightly increasing with decreasing periods, while for the longer waves, the values of ψ decreases rapidly with increasing periods or wave lengths. Therefore, the shorter waves which contribute to hydrodynamic roughness of the sea surface have "two-peaked" directional spectrum. This may suggest that the two-dimensional structure of sea surface, such as alternative smooth and rough portions, is attributed to the spectral characteristics of the wind waves.

A simple mathematical model will be developed for cell-like motion induced by wind blowing over alternative smooth and rough sea surface. Since the roughness of the sea surface changes wind stresses, the effect of variable roughness causes variable shearing motion of the water near the surface. It is assumed that the wind blows in x-direction causing a shear flow $U(y,z)$ which is constant in the x-direction. The z-axis is taken positive downwards, the y-axis is perpendicular to the x-axis and the origin is taken at the sea surface. Only the mean motion is considered. Then equations of motion are

$$v\frac{\partial U}{\partial y} + w\frac{\partial U}{\partial z} = \nu\nabla^2 U \qquad (1)$$

$$v\frac{\partial v}{\partial y} + w\frac{\partial v}{\partial z} = -\frac{1}{\rho}\frac{\partial p}{\partial y} + \nu\nabla^2 v \qquad (2)$$

$$v\frac{\partial w}{\partial y} + w\frac{\partial w}{\partial z} = -\frac{1}{\rho}\frac{\partial p}{\partial z} - g + \nu\nabla^2 w \qquad (3)$$

where v and w are velocity components in the y- and z- direction respectively and ν is the kinetic viscosity. Since it is assumed that the motion is uniform in the x-direction, all quantities are independent on x. The equation of continuity becomes

$$\partial v/\partial y + \partial w/\partial z = 0 \qquad (4)$$

This equation yields a stream function for v and w, such as,

$$v = -\partial\psi/\partial z \quad , \quad w = \partial\psi/\partial y \qquad (5)$$

The equation for vorticity ξ ($= \frac{\partial w}{\partial y} - \frac{\partial v}{\partial z}$) obtained by cross-differentiation of (2) and (3) is

$$-\frac{\partial\psi}{\partial z}\frac{\partial\xi}{\partial y} + \frac{\partial\psi}{\partial y}\frac{\partial\xi}{\partial z} = R^{-1}\nabla^2\xi \qquad (6)$$

where

$$\xi = \nabla^2\psi \qquad (7)$$

and $\nabla^2 = \partial^2/\partial y^2 + \partial^2/\partial z^2$

All quantitities in equation (6) are dimensionless and R is Reynolds' number defined as $a v_o/\nu$, where a and v_o are characteristic length and velocity, respectively. If we consider a equaling 100 m as the spacing distance of the striations and assume v_o to have an order of 1 cm/sec, the order of $R = 10^5$ for the molecular viscosity equaling 0.1 cm^2/sec. Therefore, equation (6) and corresponding equation (1) can be expanded in a series of powers of R^{-1}.

(Since the wind-driven current is turbulent, it might be contended that eddy viscosity should be used for ν instead of molecular viscosity. Even so, the eddy viscosity has an order of magnitude of

10^2 cm^2/sec when Thorade's formula (Defant, 1961, p. 104) for eddy viscosity due to wind current is applied, or of 10^3 cm^2/sec when Richardson's 4/3-power law (Defant, ibid, p. 390) is applied. Therefore, R has an order of 10 to 10^2 and the expansion with R^{-1} seems to be reasonable.)

The zeroth order term of equation (10) is

$$-\frac{\partial \psi}{\partial z}\frac{\partial \zeta}{\partial y}+\frac{\partial \psi}{\partial y}\frac{\partial \zeta}{\partial z}=0 \qquad (8)$$

Corresponding term for equation (1) is obtained by substituting J into ζ of (8). This indicates that the velocity u and vorticity are expressed by

$$J=f(\psi) \quad ; \quad \zeta=F(\psi) \qquad (9)$$

where f and F are arbitrary functions.

When a rectangular cell is considered, the boundary conditions for ψ are as follows:

$$v=-\partial\psi/\partial z=0 \qquad \text{at } y=0 \text{ and } y=1 \qquad (10)$$

$$w=\partial\psi/\partial y=0 \qquad \text{at } z=0 \text{ and } Z=d \qquad (11)$$

where d is a dimensionless depth of the lower boundary. These conditions can be represented by a simple relation

$$\psi=0 \qquad \text{at } y=0 \text{ and } y=1 \text{ and } z=0 \quad Z=d \qquad (12)$$

Immediate result from equation (9) and (12) is that at the surface (z = 0)

$$\frac{\partial U}{\partial z}=\left(\frac{df}{d\psi}\right)_{\psi=0}\frac{\partial \psi}{\partial z}=const.\ v_{z=0} \qquad (13)$$

In other words, the vertical shear of U at the surface is proportional to

the lateral velocity at the surface. This indicates that the vertical shear is the strongest at the center of a cell with one gyre and it vanishes at the boundaries y = 0 and 1. (Fig. 7) Therefore, the slicks which may reduce shear near the surface may correspond to either divergence or convergence.

As a simple example, the function $F(\psi)$ is assumed as a linear function of ψ. Then the equation for x of (9) becomes

$$\nabla^2 \psi = a\psi - b \tag{14}$$

By choosing a and b arbitrarily, various types of streamlines can be obtained from the solution of (14) under the boundary condition (2). The solution is expressed by

$$\frac{a\psi}{b} = 1 - \frac{\sin\sqrt{a}\,y}{\sin\sqrt{a}} - \frac{\sin\sqrt{a}\,(1-y)}{\sin\sqrt{a}} + \sum_{n=1}^{\infty} \frac{k_n \sin n\pi y}{\sinh p_n l} \left\{ \sinh p_n (l-z) - \sinh p_n z \right\} \tag{15}$$

where

$$p_n^2 = a + (n\pi)^2 \tag{16}$$

and

$$k_n = \frac{2}{n\pi} \left\{ (-1)^{n-1} \right\} + \frac{2n\pi (\cos\sqrt{a} - 1)}{n^2\pi^2 - a} \tag{17}$$

In expression (15), the sine terms including $\sqrt{a}$ should be replaced with terms such as $\sinh\sqrt{-a}$ etc, if a is negative. Some examples of streamlines determined from equation (15) are shown in Fig. 7.

Fig. 7

Stream Function (: |/b) from Equation (1.5)

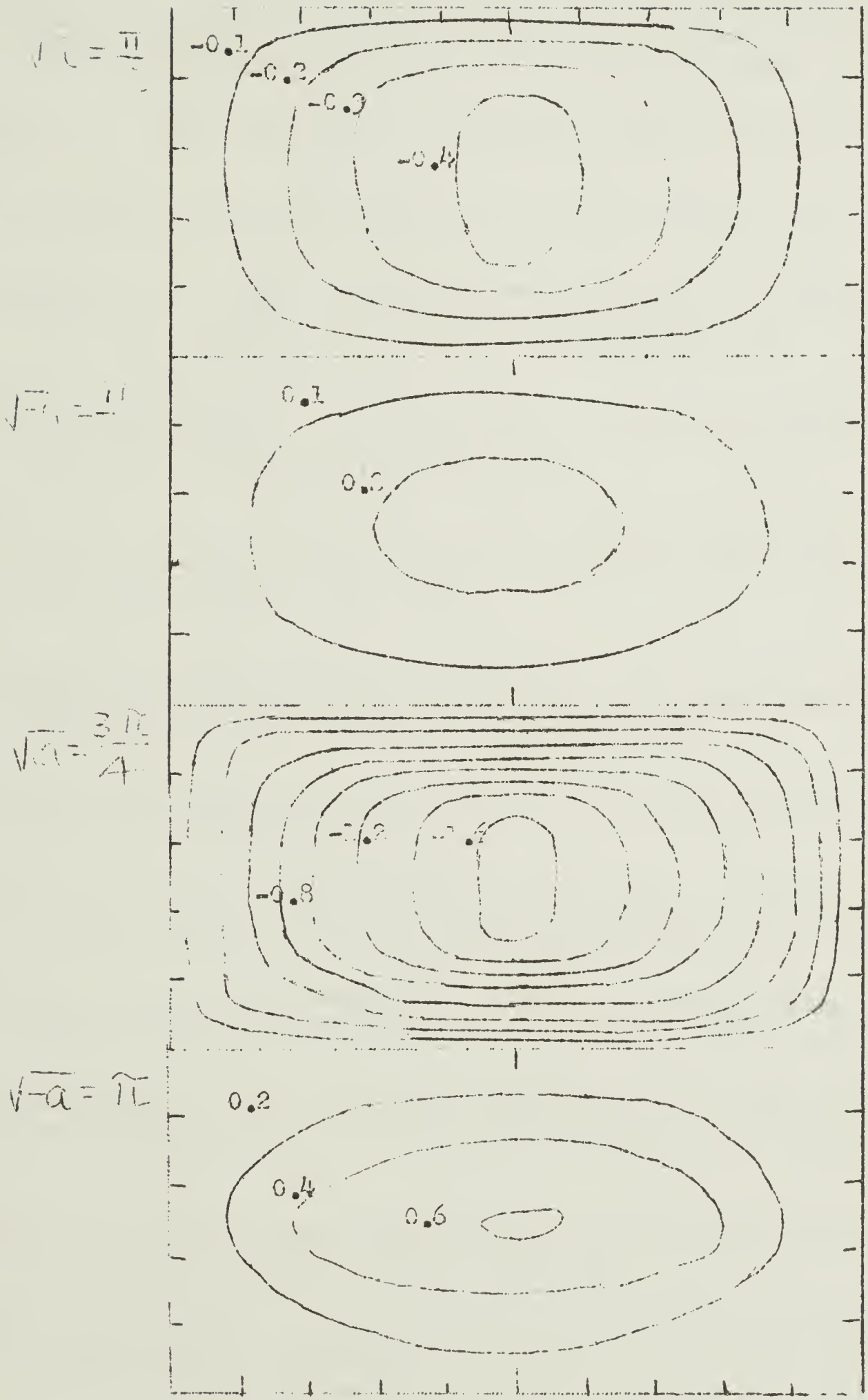

References

Costin, M., P. Davis, R. Gerard and B. Katz, 1963: Dye Diffusion Experiments in the New York Bight. Tech. Rep. No. CU-2-63, Lamont Geological Observatory (unpublished manuscript)

Defant, A., 1962: Physical Oceanography, Vol. 1 Pergamon Press

Dobroklonsky, S. V. 1947: Turbulent Viscosity in the Surface Layer of the Sea and Swell. Doklady Akad. Nauk. USSR 58(7)

Fjeldstadt, J. E. 1929: Ein Beitrage zur Theorie der Winderzeugten Meeresströmungen. Gerl. Beitr. Geophys. 23, 237

Gerard, R. and B. Katz, 1963: A Note on Some Observations of Dye in Coastal Waters Tech. Rep. No. CU-3-63 Lamont Geological Observatory (unpublished manuscript)

Ichiye, T., 1962 Oceanic Turbulence (Review) Technical Paper No. 2 for Office of Naval Research, Fla. St. Univ. Oceanog. Inst. (Unpublished manuscript)

Ichiye, T., H. Iida and and N. E. Plutchak, 1964 Analysis of Diffusion of Dye Patches in the Ocean. Tech. Rep. No. CU-8-64 Lamont Geol. Obs. (Unpublished manuscript)

Jahnke, E. and F. Emde, 1945 Tables of Functions with Formulae and Curves, Dover Publications

Kozlov, V.F. 1963, On the Influence of a Change in Vertical Mixing on Drift Currents. Izvestiya Akad. Nauk. USSR, 1963 No. 7

Lighthill, M. J., 1962 Physical Interpretation of the Mathematical Theory of Wave Generation by Wind, J. Fluid Mech. 14, 385-398

Longuet-Higgins, M.S., D.E. Cartwright and N.D. Smith, 1963 Ocean Wave Spectra, Proceedings of a Conference, Prentice-Hall, Inc. 111-136

Miles, J. W. 1960 On the Generation of Surface Waves by Turbulent Shear Flows, J. Fluid Mech. 7, 469-478

Phillips, O.M. 1957 On the Generation of Waves by Turbulent Wind. J. Fluid Mech. 2, 417-445

Shebalin, O.D. 1957 Eddy Viscosity Induced by Waves in a Shallow Sea. Trudy Akad. Nauk. USSR 116(4), 591 859-862((English Translation)

References (cont'd.)

Sverdrup. H.O. et al 1946 The Oceans pp. 1060 Prentice-Hall, Inc.

Welander, D. 1963 On the Generation of Wind Streaks on the Surface by Action of Surface Film. Tellus 15, 33-43